Indoor Planning and Optimization of LTE-U Radio Access over WiFi

Omar Sandoval[1], David González G.[1], Jyri Hämäläinen[1], Sangjo Yoo[2]
[1] School of Electrical Engineering, Aalto University, Finland
{omar.sandovalmendoza, david.gonzalezgonzalez, jyri.hamalainen}@aalto.fi
[2] Gwangju Institute of Science and Technology (GIST), Republic of Korea, asapyoo@gist.ac.kr

***Abstract*—The pursuit of more bandwidth and more efficient spectrum usage has led to consider the use of Long Term Evolution (LTE) technology in unlicensed frequency bands, a concept known as LTE-Unlicensed (LTE-U). This feature would be especially useful in *hot-spots* and indoors, where short-range pico-base stations could be used. However, indoor WiFi on unlicensed bands calls for coexistence mechanisms between LTE and WiFi. Accordingly, methods including listen-before-talk, advanced channel selection, duty-cycle, and variations of them, have been proposed. While these protocols are of great importance, we are approaching the coexistence issue from the radio access planning/optimization point of view by presenting a statistical system model for LTE-U indoor planning. The proposed optimization framework allows to obtain network topologies that maximize the benefits from the LTE-U deployment and fulfill coverage criteria. The performance of the statistically-optimized network topologies has also been validated by means of system level simulations.**

***Index Terms*—Unlicensed Spectrum, Indoor, Planning, LTE, LTE-U, WLAN, WiFi Multiobjective Optimization.**

I. Introduction

Nowadays, mobile devices are the preferred way to access the Internet [1]. The reason is the increasingly fast development of web-enabled devices, such as smartphones, tablets, and laptops. The situation has created enormous pressure on operators and manufacturers who are looking forward to 1) increase the capacity of their networks, and 2) build the fifth generation (5G) of mobile communications in order to deal with this exponential growth of the service demand.

One fundamental approach to increase the capacity of mobile networks is to use more bandwidth, but unfortunately bandwidth is a very scarce resource. Thus, millimeter-wave (mmW) communications [2] are getting significant attention because the required spectrum is in the frequency bands above 6 GHz. Besides technical challenges, spectrum harmonization also needs to be considered before the utilization of mmW. Nevertheless, in the last World Radiocommunication Conference (WRC) of the International Telecommunications Union (ITU), there was no agreement on frequency bands for mobile systems above 6 GHz. As a result, there is more pressure in the short term for optimizing the use of the spectrum below 6 GHz, in particular, the *unlicensed* one [3]. Essentially, unlicensed spectrum does not require authorization to be used, and only few restrictions exist, mainly in terms of transmit power. As it has been demonstrated by the success of Wireless Local Area Networks (WLAN), such as WiFi [4], unlicensed spectrum is suitable for indoors, i.e., short-range wireless systems.

Since indoor coverage from micro/macro cells is quite limited, especially at high frequencies, the idea of dedicated radio access based on Long Term Evolution (LTE), using unlicensed spectrum [5], has been adopted by the 3rd Generation Partnership Project (3GPP). This concept, standardized in Release 13 as *Licensed Assisted Access* (LAA) [5], will operate in the 5 GHz band, and it is also known as LTE-Unlicensed (LTE-U), which is the terminology used herein. Given that a significant part of the service demand is originated from indoors, this concept is expected to play a key role in 5G [6]. However, one fundamental issue with LTE-U is the coexistence with WiFi [3], mainly due to the differences in the design of their Medium Access Control (MAC) schemes. While LTE uses a centralized scheme that can cope with Intercell Interference (ICI), WiFi implements a distributed contention-based MAC, to avoid collisions. Thus, without proper coexistence schemes, LTE-U would jeopardize severely the performance of WiFi. To cope with this problem, several alternatives (operating in frequency and/or time domain) have been proposed:

- ✓ *Dynamic Channel Selection* (DCS): where the idea is to search and take a *free* channel,
- ✓ *Listen-Before-Talk* (LBT): where a channel is taken only if it is *clear*, i.e., not being used,
- ✓ *Duty Cycle* (DC): where a channel is taken and released periodically, and
- ✓ *Power Control* (PC): where transmit power is adjusted based on certain criteria.

Table I provides a summary of some recent representative contributions. As can be seen in Table I, most of the related works focuses on performance assessments and mechanisms to improve coexistence by means of the aforementioned schemes: either combinations and/or variations of them. Modeling and analysis of the basic coexistence schemes have already been addressed from different angles, although this issue is relatively new. This paper makes a contribution by looking at this problem from a different perspective: the network planning and radio access optimization point of view. As it was mentioned, WiFi is a successful technology that is everywhere, and will continue being there. Therefore, although coexistence schemes exist, effective planning and radio access optimization

TABLE I
SUMMARY OF RELATED WORK.

Ref.	Test-case	Scheme	Planning	Method
[3]	LTE-U/WiFi: Indoors	DC + PC	×	S
[5]	LTE-U/WiFi: HetNets	DC	×	S
[7]	LTE-U/LTE-U: Outdoors	DC-based	×	S
[8]	LTE-U/WiFi: Outdoors	DC+PC	×	S + A
[9]	LTE-U/WiFi: Both	DCS+PC	×	S + A
[10, 11]	LTE-U/WiFi: Both	LBT-based	×	A
[12]	LTE-U/WiFi: Indoor	DCS-based	×	S + A
[13]	LTE-U/WiFi: Both	LBT-DCS	×	S + A
[14]	LTE-U/WiFi: Indoor	PC	×	S
[15]	LTE-U/WiFi: Indoor	DC+LBT	×	A + S
[16]	LTE-U/WiFi: Indoor	DC-based	×	A

S: Simulations, A: Analytic

are complementary tools to make them more effective, and eventually, get the most benefits from both systems. Herein, we address the problem of optimally deploying a set of LTE-U Access Points (APs) in a given indoor environment where WiFi is already deployed. The contribution of this paper is to present a framework for LTE-U indoor planing and optimization based on a statistical system model that allows efficient assessment of LTE-U network topologies, given the operation of WiFi and coexistence requirements (based on LBT). Other schemes, such as DC, can also be considered within this framework. Required inputs include the characteristics of the radio propagation, the statistical description of the service demand, and the preferences of the network operator. The output is a set of optimized network topologies that can be used to plan or optimize the indoor deployment.

The rest of the paper is organized as follows: the next section provides a high level description of the proposed framework. The statistical system model and the proposed optimization formulation are presented in Sections III and IV, respectively. Section V provides the numerical results, and Section VI closes the paper with the conclusions.

II. PROPOSED FRAMEWORK

Radio access planning is about determining the number of APs and their locations to satisfy a certain service demand. In this framework, this is done by means of a statistical model that captures the behavior, performance, and coexistence of both systems (LTE-U and WiFi). Fig. 1 provides a big picture of the proposed framework, composed of 5 stages:

1) *Radio propagation characterization*: The first stage is modeling the radio propagation. In order to do this in indoor environments, it is essential to consider actual building structures, layouts, and materials. Nowadays, deterministic methods based on Ray-Tracing (RT) [17] and/or Laser scanning [18] are the most accurate approaches, and their use is very popular due to the increasing availability of very detailed 3D models and databases. Indeed, these techniques are also accurate for higher frequencies, and hence, the advent of millimeter waves is likely to popularize these methods, especially indoors, where penetration losses significantly affect the coverage [19].
2) *System model*: This phase comprises developing a mathematical model that can be efficiently used for optimization purposes; the main goal is to capture the behavior and performance of both systems, in statistical terms. The proposed statistical model is presented in Section III.
3) *Performance metrics and optimization*: In this phase, the objective is to define the performance indicators to be optimized (typically defined by the network operator), and the type of optimization that is required. The proposed optimization formulation is presented in Section IV.
4) *System Level Simulations* (SLS): Detailed system level trials are required to validate the performance of the optimized topologies. Since it is not possible to model mathematically many features of real systems, SLS are always required once the radio access network is defined. We also note that SLS provide means to fine-tune the statistical model if the behavior of some performance indicator is not satisfactory at the system level.
5) *Application*: Optimized/validated network topologies can be used for new deployments. These configurations can also be used in conjunction with *Cloud*-Radio Access Network (C-RAN) [20] to perform real-time topology adaptation or Cell Switch-Off (CSO) [21, 22].

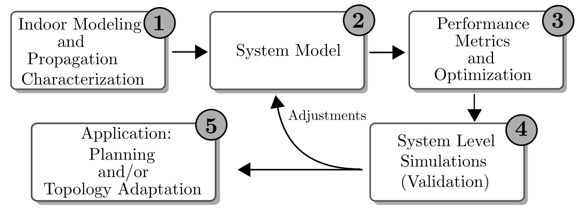

Fig. 1. Framework for planning and optimization of LTE-U deployments.

III. SYSTEM MODEL

The downlink of an Orthogonal Frequency Division Multiple Access (OFDMA), representing the LTE-U network, is considered. As in LAA, the uplink is assumed to be transmitted in licensed bands, and hence, it is not considered. WiFi employs Time Division Multiple Access (TDMA) with Time Division Duplex (TDD). Both networks are assumed to use the same channel[1] with bandwidth B_{ch}. The WiFi deployment is composed of L_{W} APs. There are L_{L} LTE-U candidate locations. The (indoor) coverage area $\mathcal{A}$ is the same for both networks and it is divided into A small area elements in which the received power is constant, and hence, the Signal-to-Interference plus Noise Ratio (SINR) is also constant. The indexes of the area elements corresponding to the l^{th} and i^{th} LTE-U and WiFi AP are a_{L}^{l} and a_{W}^{i}, respectively. The APs have omnidirectional antennas and they transmit the same power, i.e., P_{L}^{tx} and P_{W}^{tx}, for LTE-U and WLAN, respectively.

The radio propagation, i.e., path loss and antennas' gain, is represented by the matrices $\mathbf{G}_{\text{L}} \in \mathbb{R}^{A \times L_{\text{L}}}$ and $\mathbf{G}_{\text{W}} \in \mathbb{R}^{A \times L_{\text{W}}}$, for LTE-U and WiFi, respectively. The vector $\mathbf{x} \in \{1, 0\}^{L_{\text{L}}}$ determines the '*topology*' of the LTE-U network, i.e., if the l^{th} candidate location has an LTE-U AP, then $\mathbf{x}(l) = 1$, and 0 otherwise. Given that the objective is to determine the

[1]The general case where several channels are available will be addressed in future as a generalization of this study.

best locations for the LTE-U nodes, $\mathbf{x}$ is the optimization variable. Cell selection in the LTE-U network is based on average Pilot Signals (PS) received power. Therefore, the matrix $\mathbf{R}_{\text{PS}} \in \mathbb{R}^{A \times L_{\text{L}}}$, indicating the received power in each area element, can be computed as follows:

$$\mathbf{R}_{\text{PS}}(\mathbf{x}) = \mathbf{G}_{\text{L}} \cdot \operatorname{diag}(\mathbf{p}_{\text{PS}} \odot \mathbf{x}), \tag{1}$$

where $\mathbf{p}_{\text{PS}} \in \mathbb{R}^{L_{\text{L}}}$ indicates the transmit power in PS. The operators $\odot$ and $\oslash$ indicate Hadamard (pointwise) operations for multiplication and division, respectively. Note that the dependence of $\mathbf{R}_{\text{PS}}$ on $\mathbf{x}$ is explicitly indicated. Hereafter, this dependence will be omitted for the sake of clarity. Hence, the a^{th} area element (a^{th} row in $\mathbf{R}_{\text{PS}}$) will be served by cell $l^\star$ if:

$$l^\star = \underset{l \in \{1,2,\dots,L_{\text{L}}\}}{\operatorname{argmax}} \mathbf{R}_{\text{PS}}(a,l). \tag{2}$$

Equations 1 and 2 can be used to built the (binary) coverage matrices $\mathbf{S}$ and $\mathbf{S}^{\text{c}} \in \{0,1\}^{A \times L_{\text{L}}}$. In this manner, if $\mathbf{S}(a,l^\star) = 1$, the a^{th} area element is served by AP $l^\star$. $\mathbf{S}^{\text{c}}$ is the binary complement of $\mathbf{S}$. Herein, it is assumed that each area element is only served by one AP. The vector $\mathbf{\Gamma} \in \mathbb{R}^A$ contains the SINR in each pixel, and it is given by

$$\mathbf{\Gamma} = \mathbf{P}^{\text{u}} \oslash \left[\, \mathbf{I}_{\text{L}} + \mathbf{I}_{\text{W}} + \boldsymbol{\sigma}^2 \,\right]. \tag{3}$$

$\mathbf{P}^{\text{u}}$, $\mathbf{I}_{\text{L}}$, $\mathbf{I}_{\text{W}}$, and $\boldsymbol{\sigma}^2$ (all $\in \mathbb{R}^A$) correspond to the power received from the serving LTE-U node, the interference generated by the LTE-U network, the interference coming from the WiFi network, and the noise power, respectively. In this case, $\mathbf{P}^{\text{u}} = (\mathbf{S} \odot \mathbf{G}_{\text{L}}) \cdot (\mathbf{p}_{\text{D}} \odot \mathbf{x})$ and $\mathbf{I}_{\text{L}} = (\mathbf{S}^{\text{c}} \odot \mathbf{G}_{\text{L}}) \cdot (\mathbf{p}_{\text{D}} \odot \mathbf{x})$. The vector $\mathbf{p}_{\text{D}} \in \mathbb{R}^{L_{\text{L}}}$ gives the transmission power of each LTE-U AP in the data channel. Herein, $\mathbf{p}_{\text{D}}(l) = \mathbf{p}_{\text{PS}}(l) = P_{\text{L}}^{\text{tx}}$, $\forall\, l = \{1,2,...,L_{\text{L}}\}$. The expression for $\mathbf{I}_{\text{W}}$ is provided later on.

It is considered that the a^{th} area element has coverage if the SINR and received power are greater than certain thresholds, i.e., $\mathbf{\Gamma}(a) \geq \gamma_{\min}$ and $\mathbf{R}_{\text{PS}}(a,l^\star) \geq P_{\min}$ are satisfied. Thus, in order to integrate these coverage criteria (to penalize topologies with coverage holes), the spectral efficiency of each area element is stored in the vector $\boldsymbol{\eta} \in \mathbb{R}^A$ and it is given by

$$\boldsymbol{\eta}(a) = \mathbf{c}(a) \cdot f_{\text{Link}}\left(\, \mathbf{\Gamma}(a) \,\right), \tag{4}$$

where each element of $\mathbf{c} \in \mathbb{R}^A$ is computed as follows:

$$\mathbf{c}(a) = \mathrm{u}\left(\mathbf{\Gamma}(a) - \gamma_{\min}\right) \cdot \mathrm{u}\left(\mathbf{R}_{\text{PS}}(a,l^\star) - P_{\min}\right). \tag{5}$$

The mapping $f_{\text{Link}} : \mathbb{R}_+ \to \mathbb{R}_+$ [bps/Hz] corresponds to the link performance model and it is usually assumed to be a nondecreasing function of the SINR. In (5), $\mathrm{u}(x)$ is the unit step function and it is defined as follows: $\mathrm{u}(x) = 1$ if $x \geq 0$, and 0 otherwise. Recall that $l^\star$ is the index of the LTE-U node serving the a^{th} area element.

In order to built the system model, it is considered that the service demand is known in statistical terms [23, 24]. In the LTE-U network, the service demand is modeled in terms of volume (M) and spatial distribution (δ_{L}). M corresponds to the average number of users in the system. It can be obtained by considering inter-arrival and session times, λ and μ, respectively, as random variables. Thus, $M = \frac{\mathbb{E}\{\mu\}}{\mathbb{E}\{\lambda\}}$. δ_{L} is a Probability Density Function (PDF) that gives the probability of each pixel $a \in \mathcal{A}$ of having a user on it. Hence, $\int_{\mathcal{A}} \delta_{\text{L}}(a)\, da = 1$, and obviously $\delta_{\text{L}}(a) \in [0,1]$, $\forall a \in \mathcal{A}$. It is possible to write δ_{L} as a vector, and hence, the notation $\boldsymbol{\delta}_{\text{L}} \in \mathbb{R}^A$ is also used. Since WiFi is already deployed, traffic statistics are available, i.e., average load ($\alpha \in [0,1]$) and traffic asymmetry ($\rho \in [0,1]$), per access point. In case of TDD systems, the average load corresponds to the fraction of time with transmissions, either downlink or uplink. The fraction of this *activity* time allocated to downlink transmissions corresponds to ρ. Hence, if for a certain period of time, $\alpha_i \triangleq \mathbb{E}\{\alpha_i(t)\} = 0.6$ and $\rho_i = 0.7$, then the i^{th} WiFi AP and its users use the channel 60% of the time, of which 70% corresponds to downlink transmissions. Thus, the AP is transmitting 42%, receiving 18%, and leaving the channel clear 40% of the time. In order to take into account the uplink interference created by WiFi users, a spatial service demand distribution can be defined. Similarly to LTE-U, a vector $\boldsymbol{\delta}_{\text{W}} \in \mathbb{R}^A$ representing the spatial service demand distribution is considered. The notation α_x is used to denote the average load of both LTE-U and WiFi APs[2]. The meaning will be clear from the context, otherwise it will be explicitly indicated. Traffic asymmetry figures only apply to WiFi.

Since LBT is considered, Clear Channel Assessment (CCA) needs to be carried out. Cellular networks are designed to operate under full frequency reuse conditions, with potentially high levels of ICI, hence, CCA is based on the interference received from the WiFi network. Thus, the interference received at the l^{th} LTE-U AP, at time t, is given by

$$I_l(t) = \sum_{i=1}^{L_{\text{W}}} z_i(t) \left[I_{i,l}^{\text{d}}(t) + I_{i,l}^{\text{u}}(t) \right]. \tag{6}$$

The z_i's are Bernoulli random variables to model the channel occupancy of the i^{th} WiFi AP at time t. Since its average load is known and given by α_i, then $\mathbb{E}\{z_i(t)\} = \alpha_i$. The terms $I_{i,l}^{\text{d}}$ and $I_{i,l}^{\text{u}}$ correspond to downlink and uplink transmissions associated to the i^{th} WiFi AP. These are given as follows:

$$I_{i,l}^{\text{d}}(t) = P_{\text{W}}^{\text{tx}} \cdot \mathbf{G}_{\text{W}}(a_{\text{L}}^{l}, i) \cdot \chi_i(t), \tag{7}$$

and

$$I_{i,l}^{\text{u}}(t) = P_{\text{W}}^{\text{tx,u}} \cdot [1 - \chi_i(t)] \cdot \sum_{a \in \mathcal{A}_{\text{W}}^{i}} \frac{\boldsymbol{\delta}_{\text{W}}(a) \cdot \mathbf{G}_{\text{L}}(a,l)}{\sum_{a' \in \mathcal{A}_{\text{W}}^{i}} \boldsymbol{\delta}_{\text{W}}(a')}. \tag{8}$$

The χ_i's are also Bernoulli random variables to model the TDD behavior of WiFi as well as the traffic asymmetry. Hence, $\mathbb{E}\{\chi_i(t)\} = \rho_i$. The random variables χ_i and z_i are independent. It is considered that the interference generated by WiFi comes either from downlink or uplink. The case of collisions, when both happens at a time, is left for future study as this generalization makes the model significantly more complex (collision probability also depends on load, among other aspects). The average uplink interference received at the l^{th} LTE-U AP, generated from the coverage of the i^{th} WiFi

[2]The notion of load in LTE-U APs is similar to WiFi, it refers to the (average) fraction of resources required to satisfy the service demand [25].

AP ($\mathcal{A}_{\mathrm{W}}^{i}$), is obtained by considering the transmit power of WiFi users ($P_{\mathrm{W}}^{\mathrm{tx,u}}$) and their average channel gains, i.e., the sum indicated in (8). Thus, the probability of having positive clear channel assessment ($P^{\mathrm{CAA+}}$) is the probability that an LTE-U AP receives WiFi interference below a certain threshold, i.e., for the l^{th} LTE-U AP at time t

$$P_{l}^{\mathrm{CAA+}}(t) = \mathrm{P}\left(I_l(t) < I_{\mathrm{CCA}}^{\mathrm{TH}} \right). \tag{9}$$

Finally, to complete the system model, the term $\mathbf{I}_{\mathrm{W}}$ in (3) is required. $\mathbf{I}_{\mathrm{W}}(a)$ corresponds to the average interference received in the $a^{\mathrm{th}} \in \mathcal{A}_{\mathrm{L}}^{l}$ area element from the WiFi network when obviously $\mathbf{x}(l) = 1$, and the AP obtains positive CCA. $\mathcal{A}_{\mathrm{L}}^{l}$ is the set of area elements associated to the l^{th} LTE-U AP. Again, both downlink and uplink components of the interference need to be considered, therefore

$$\mathbf{I}_{\mathrm{W}}(a) = I_{\mathrm{W}}^{\mathrm{d}}(a) + I_{\mathrm{W}}^{\mathrm{u}}(a), \tag{10}$$

where

$$I_{\mathrm{W}}^{\mathrm{d}}(a) = \sum_{i=1}^{L_{\mathrm{W}}} \left[P_{\mathrm{W}}^{\mathrm{tx}} \cdot \mathbf{G}_{\mathrm{W}}(a,i) \cdot \mathbb{E}\{ z_i \chi_i \,|\, \mathrm{CCA+}^{(l^\star)} \} \right], \tag{11}$$

and

$$I_{\mathrm{W}}^{\mathrm{u}}(a) = \sum_{i=1}^{L_{\mathrm{W}}} \sum_{a' \in \mathcal{A}_{\mathrm{W}}^{i}} \left[P_{\mathrm{W}}^{\mathrm{tx,u}} \cdot \frac{\boldsymbol{\delta}_{\mathrm{W}}(a') \cdot \mathbf{G}(a',a)}{\sum_{a'' \in \mathcal{A}_{\mathrm{W}}^{i}} \boldsymbol{\delta}_{\mathrm{W}}(a'')} \cdot \quad \ldots \right.$$
$$\left. \ldots \quad \cdot \mathbb{E}\{ z_i \,(1 - \chi_i) \,|\, \mathrm{CCA+}^{(l^\star)} \} \right]. \tag{12}$$

In (11) and (12), $\mathrm{CCA+}^{(l^\star)}$ indicates the event that the LTE-U AP $l^\star$ (the one serving the a^{th} area element) obtains positive CCA. The matrix $\mathbf{G} \in \mathbb{R}^{A \times A}$ contains the full network geometry, i.e., the average channel gain of each pixel with respect to each other. Note that, indeed, $\mathbf{G}_{\mathrm{L}}$ and $\mathbf{G}_{\mathrm{W}}$ are submatrices of $\mathbf{G}$. This information is generated *offline* using measurements or simulations, but it is worth noting that $\mathbf{G}$ is *sparse* due to the high isolation of indoor environments. Hence, memory requirements are much less than $A \times A$.

In general, evaluating (9) and the conditional expectations[3] [26] in (11) and (12) is difficult, and only under very restrictive assumptions, closed forms exists. However, as these figures depends on the service demand and network geometry (both known), they only need to be (numerically) evaluated once. In this paper, the focus is placed on the important particular case of highly asymmetric traffic: the case when it can be assumed that the WiFi interference is only generated by the APs, i.e., downlink. Under this assumption, the model gets significantly simplified. Thus, if $\rho_i = 1,\ \forall\, i = 1, 2, \cdots, L_{\mathrm{W}}$, then $I_l(t)$, see (6), becomes

$$I_l(t) = \sum_{i=1}^{L_{\mathrm{W}}} z_i(t) \cdot I_{i,l}^{\mathrm{d}}(t) = \sum_{i=1}^{L_{W}} z_i(t) \cdot P_{\mathrm{W}}^{\mathrm{tx}} \cdot \mathbf{G}_{\mathrm{W}}(a_{\mathrm{L}}^{l}, i). \tag{13}$$

[3]The conditional expectation of the random variable X given the event B is defined as follows: $\mathbb{E}\{X|B\} \triangleq \sum_x x\, f(x|B)$, being $f(x|B)$ the conditional density of X given B.

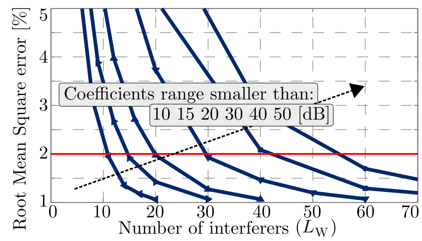

Fig. 2. Gaussian approximation: weighted sum of Bernoulli distributed independent random variables.

Similarly,

$$\mathbf{I}_{\mathrm{W}}(a) = \sum_{i=1}^{L_{\mathrm{W}}} \left[P_{\mathrm{W}}^{\mathrm{tx}} \cdot \mathbf{G}_{\mathrm{W}}(a,i) \cdot \mathbb{E}\{ z_i \,|\, \mathrm{CCA+}^{(l^\star)} \} \right]. \tag{14}$$

Therefore, the distribution of $I_l(t)$ is required. Equation 13 represents a weighted sum of Bernoulli random variables that can be approximated as a Gaussian random variable when L_{W} is large. Unfortunately, this is not always the case, but in such cases the numerical estimation of the distribution is very simple. Fig. 2 shows the Gaussian Root Mean Square (RMS) error approximation as a function of the number of interferers (L_{W}) for different ranges of the weights, i.e., the constants $P_{\mathrm{W}}^{\mathrm{tx}} \cdot \mathbf{G}_{\mathrm{W}}(a_{\mathrm{L}}^{l}, i)$ in (13). These weights represent the difference in the received power from the WiFi APs. As a reference, an RMS of 2% (which can be considered an acceptable approximation in this context) is indicated in red. Finally, regarding (14), it is easy to see that

$$\begin{aligned}
\mathbb{E}\{\, z_i \,|\, I_l(t) < I_{\mathrm{CCA}}^{\mathrm{TH}} \,\} &= P\left(z_i = 1 \,|\, I_l(t) < I_{\mathrm{CCA}}^{\mathrm{TH}} \right) \\
&= \frac{P\left(z_i = 1 \,;\, I_l(t) < I_{\mathrm{CCA}}^{\mathrm{TH}} \right)}{P\left(I_l(t) < I_{\mathrm{CCA}}^{\mathrm{TH}} \right)}
\end{aligned}$$
$$= \frac{P\left(\sum\limits_{j=1; j \neq i}^{L_{\mathrm{W}}} P_{\mathrm{W}}^{\mathrm{tx}} \cdot \mathbf{G}_{\mathrm{W}}(a_{\mathrm{L}}^{l}, j) < \left[I_{\mathrm{CCA}}^{\mathrm{TH}} - P_{\mathrm{W}}^{\mathrm{tx}} \cdot \mathbf{G}_{\mathrm{W}}(a_{\mathrm{L}}^{l}, i) \right] \right)}{P\left(I_l(t) < I_{\mathrm{CCA}}^{\mathrm{TH}} \right)}, \tag{15}$$

which can easily be evaluated for small values of L_{W}.

IV. Multiobjective Problem Formulation

The objective is to simultaneously optimize several performance metrics which are usually in conflict, i.e., improving one of them implies worsening another. Multiobjective optimization (MO) [27] is the discipline that studies the resolution of problems involving more than one *objective* function. One interesting aspect of MO is that, the solution of these types of problems is a set of solutions, rather a single optimal solution. As a set, these solutions represent the best possible tradeoff among the objective functions. This set is known as Pareto Front (PF) [28], and it offers a complete view of the context-and-problem-specific tradeoffs.

Herein, our interest is on maximizing the aggregate capacity of the LTE-U network for a given number of APs, subject to the presence of WiFi and a minimum required coverage. Thus, taking into account the previously introduced system model, the following two objective functions are defined:

$$f_1(\mathbf{x}) = \mathbf{x} \cdot \mathbf{1}, \tag{16}$$

that corresponds to the number of LTE-U APs in a certain topology $\mathbf{x}$, and

$$f_2(\mathbf{x}) = (B_{\text{ch}} \cdot A) \left[\left[(\boldsymbol{\eta} \odot \boldsymbol{\delta}_{\text{L}})^{\text{T}} \cdot \mathbf{S} \right] \odot \mathbf{n} \odot \mathbf{P}^{\text{CAA+}} \right] \cdot \mathbf{1}, \quad (17)$$

that corresponds to the sum of average capacity of the LTE-U APs; the dependence on $\mathbf{x}$ is implicit in (17) as $\boldsymbol{\eta}$ and $\mathbf{S}$ depend on $\mathbf{x}$, see (1), (2), and (4). The vector $\mathbf{n} \in \mathbb{R}^{L_{\text{L}}}$ indicates the inverse of the number of area elements served/associated to each LTE-U AP. It is adopted by convention that if $\mathbf{x}(l) = 0$, then $\mathbf{n}(l) = 1$ because in such cases, the l^{th} element of the vector $(\boldsymbol{\eta} \odot \boldsymbol{\delta}_{\text{L}})^{\text{T}} \cdot \mathbf{S}$, that represents the average capacity of each AP, is also zero. The joint use of $\boldsymbol{\delta}_{\text{L}}$ and A in (17) captures the impact of the spatial distribution of the service demand on the resulting average capacity, by weighting more the area elements where traffic is more likely to appear. The use of $\mathbf{P}^{\text{CAA+}} \in \mathbb{R}^{L_{\text{L}}}$ scales the achievable rate of each AP by its probability of having positive CCA. Thus, $\mathbf{P}^{\text{CAA+}}$ is created directly by evaluating (9) for each l, independently of the value of $\mathbf{x}(l)$. This only needs to be done once because $\mathbf{P}_l^{\text{CAA+}}$ only depends on the WiFi network load (the α_i's) and network geometry. All together, f_2 represents the aggregate capacity of the LTE-U deployment specified by $\mathbf{x}$, and its unit is bps as it is considered that the whole channel bandwidth B_{ch} is reused in each LTE-U AP, so full reuse is assumed.

Thus, proposed multiobjective optimization problem can be written as follows:

$$\underset{\mathbf{x}}{\text{minimize}} \quad \mathbf{f} = [\ f_1(\mathbf{x}),\ \ -f_2(\mathbf{x})\ ], \quad (18a)$$

subject to:

$$O_{\max} \ \geq \ 100 \cdot \left(1 - \left[\left(\mathbf{c}^{\text{T}} \cdot \mathbf{1} \right) \cdot A^{-1} \right] \right), \quad (18b)$$

$$\mathbf{x} \in \{0,1\}^L, \ \mathbf{x} \neq \mathbf{0}. \quad (18c)$$

Conditions (18b) and (18c) correspond to the maximum allowed outage ($O_{\max}$) and the *search space* of $\mathbf{x}$, respectively. The problem given in (18) is NP-complete, and due to the mathematical structure of f_2 (with local optima), the use of metaheuristics [28] is proposed. Herein, the Nondominated Sorting Genetic Algorithm II (NSGA II) [29] has been employed. Calibration and some additional guidelines are provided in Section V-A.

V. Numerical Results

A. Evaluation Setting

The test-case considered for numerical evaluations is the 1st floor of the School of Electrical Engineering at Aalto University, Finland, as shown in Fig. 3. Existing WiFi APs are indicated by red circles while blue triangles indicate the candidate locations for LTE-U APs. The radio propagation, i.e., the matrices $\mathbf{G}_{\text{W}}$, $\mathbf{G}_{\text{L}}$, and $\mathbf{G}$, has been obtained using a commertial 3D Ray-tracing tool [30]. A certain irregular distribution for the service demand has been assumed in this exercise, and it is indicated as δ_{L} in Fig. 3. The rest of the parameters and assumptions, including the calibration of the algorithm NSGA-II [29], are indicated in Table II.

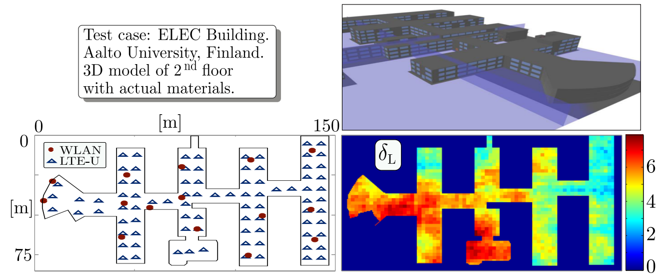

Fig. 3. Test case for numerical evaluation.

TABLE II
Simulation Parameters and Evaluation Setting.

System model			
L_{L}	87	L_{W}	15
Area elements	$0.5 \times 0.5\,\text{m}^2$	A	20968
Tx. power: $P_{\text{L}}^{\text{tx}}/P_{\text{W}}^{\text{tx}}$	15 / 17 dBm	σ^2	-174 dBm/Hz
SINR min ($\gamma_{\min}$)	-7 dB	Sensitivity ($P_{\min}$)	-126 dBm/PS
Link: $f_{\text{Link}}(\gamma)$	$\log_2(1+\gamma)$	CCA+ ($< I_{\text{CCA}}^{\text{TH}}$)	-94.75 dBm
B_{ch}	20.0 MHz	δ_{L} (see Fig. 3)	Non-uniform
Antennas	Omni	Antennas gain	3 dBi
Antennas height	3.5 m	Coverage ($O_{\max}$)	98%
LTE-based system level simulations			
Resource blocks	100	Scheduler	[31]
Traffic model	FTP [32]	Target rate R_{TH}	1 Mbps
Carrier freq. (f_c)	5.7 GHz	Channel feedback	Ideal
Calibration of the algorithm NSGA-II			
Population size	110	Crossover prob.	1.00
Type of variables	Discrete	Mutation prob.	$1/L_{\text{L}}$
Termination criterion:	*hypervolume* [27] gain $< 0.001\%$ (40 generations).		

B. Multiobjective Evolutionary Optimization

The solutions of (18) through multiobjective evolutionary optimization are presented in Fig. 4. Three different WiFi load patterns have been considered: two cases where the APs have the same load (pattern *low* (L): $\alpha_i = 0.25$, and pattern *high* (H): $\alpha_i = 0.75$, $\forall\, i$), and a case where the load of each AP is different (pattern *intermediate* (I): $\alpha_i \in [0.1, 0.9]$). As previously indicated, it is assumed that there is only downlink traffic, thus $\rho_i = 1, \forall\, i$. These patterns are shown in Fig. 4a. Fig. 4b shows the performance (f_1 vs. f_2) of the resulting set of Pareto efficient topologies for each load pattern. The proposed statistical model succeeds in capturing the behavior found in practice: under the assumption that the LTE-U APs implement LBT, the higher the load of the WiFi network, the lower the achievable capacity. This is because heavy WiFi loads reduce the probability of positive CCA in the LTE-U APs, on average. In order to illustrate this, Fig. 4c shows the resulting empirical distribution of $P^{\text{CCA+}}$, see (9), for the patterns L, I, and H, using the optimized topologies with 26 nodes, $\mathbf{x}_{26}^{L}$, $\mathbf{x}_{26}^{I}$, and $\mathbf{x}_{26}^{H}$, respectively, as an example. These network configurations are also shown in Fig. 4d. Under load pattern H, the average $P^{\text{CCA+}}$ of $\mathbf{x}_{26}^{H}$ is 0.51 and $f_2 = 1.81\,\text{Gbps}$. If the overall WiFi load is reduced as in pattern I, then the optimal topology $\mathbf{x}_{26}^{I}$ obtains more *air-time* (from 0.51 to 0.66) with its corresponding capacity gain of 35.4% (f_2 from 1.81 to 2.45 Gbps). If WiFi load is further reduced to load pattern L, then $\mathbf{x}_{26}^{L}$ increases its *air-time* from 0.66 to 0.88 and gains 18% in terms of f_2 (from 2.45

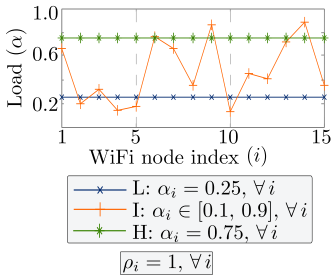

(a) WLAN load patterns

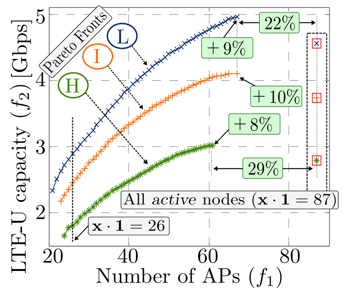

(b) Pareto efficient LTE-U topologies.

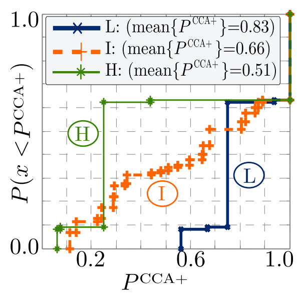

(c) CCA successful probability.

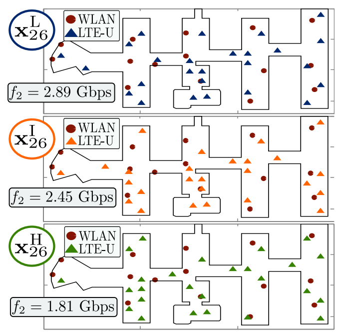

(d) Optimized LTE-U topologies.

Fig. 4. Multiobjective optimization for LTE-U indoor planning.

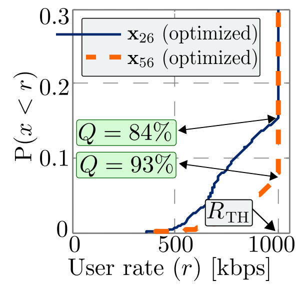

(a) CDF of users' rate.

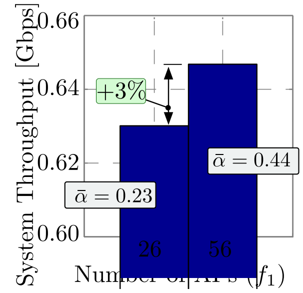

(b) System throughput

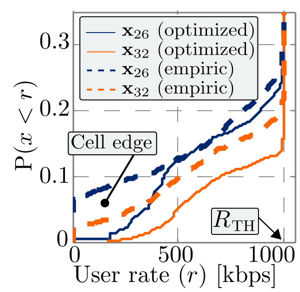

(c) CDF of users' rate.

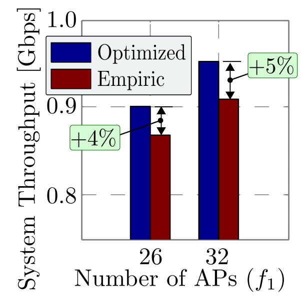

(d) System throughput

Fig. 5. Validations: system level simulations.

to 2.89 Gbps). The optimality of these topologies is not only in terms of f_1 and f_2, but also in terms of more complex metrics obtained from SLS, as it will be shown shortly. In some cases, LTE-U nodes appear close to WiFi APs, which is due to the fact that f_2 considers not only $P^{\text{CCA+}}$ (that depends on WiFi) but also the interference coming from other LTE-U nodes.

Thus, the proposed optimization framework allows not only to determine the optimal topologies for each WiFi load pattern, but also to find what is the maximum density that is worth to deploy, i.e., after a certain number of APs, the increased spatial frequency reuse is not longer the dominating effect, but the increase in terms of interference. The highest worth density (f_1) for the patterns L, I, and H, are 67, 67, and 61, respectively. This means that those topologies reduce the number of APs by 22% and 29%, and still provide capacity gains of 9%, 10%, and 8% with respect to the *all-on* topologies, indicated in red in Fig. 4b. The lowest value of f_1 indicates the minimum number of APs to provide the desired coverage level, which is highly environment-specific. Thus, the framework is versatile as it can be used for planning or to determine the best subset of APs, if the network is already deployed. In addition, other performance indicators can be defined, e.g., maximizing the throughput of the *weakest* cell (a max-min approach).

C. System Level Simulations

System level simulations were carried out using a MATLAB-based LTE-oriented simulator. The Monte-Carlo experiments with 500 independent realizations, each having 10000 Transmission Time Intervals (TTIs), in which M users were distributed according to δ_{L}, as in Fig. 3.

Figs. 5a and 5b show a comparison in terms of users' rate and system throughput, respectively. The goal is to illustrate how dominance relationships among topologies, see Fig. 4b, are also preserved at system level. Two optimized topologies with 26 and 56 APs, i.e., $\mathbf{x}_{26}^{\text{L}}$ and $\mathbf{x}_{56}^{\text{L}}$, are considered. A service demand volume $M = 650$, which can be handled by $\mathbf{x}_{56}^{\text{L}}$ in a compatible manner with the WiFi load pattern L (see Fig. 4a), has been selected to compare $\mathbf{x}_{26}^{\text{L}}$ and $\mathbf{x}_{56}^{\text{L}}$. As it can be seen, $\mathbf{x}_{56}^{\text{L}}$ not only provides better satisfaction ratio (Q) [31], i.e., the percentage of users achieving the target rate R_{TH}, but also (and more important) achieves that respecting WiFi, i.e., the resulting load of each node is below $P_l^{\text{CAA+}}$. The average load of the LTE-U APs ($\bar{\alpha}$) is indicated in Fig. 5b, where a 3% system throughput improvement is shown. Therefore, it is convenient to evaluate the set of Pareto efficient topologies using SLS (for different values of M) in order to validate the *system capacity* [31] and performance aspects, possibly in terms of other metrics.

Optimality relationships among topologies can also be verified using SLS. This is shown in Fig. 5c and 5d, where two empiric topologies, with minor variations with respect to $\mathbf{x}_{26}^{\text{L}}$ and $\mathbf{x}_{32}^{\text{L}}$, are considered. Optimized topologies performs consistently better both in terms of users' rate and system throughput. In the example, these small *topological* variations result in throughput losses of 4% and 5%. Other topologies with 26 or 32 APs result in larger losses, and unacceptable coverage outages. This was extensively verified using SLS.

Thus, the framework shown in Fig. 1 provides effective means to address 1) LTE-U topology optimization (unfeasible using SLS as there are $2^{L_{\text{L}}}$ possible topologies), and 2) accurate capacity and Quality of Service (QoS) analysis considering realistic system features (non-tractable mathematically).

VI. Conclusions

Cellular technology operating in unlicensed bands has been recognized as a key feature of current and future wireless systems. However, coexistence with WiFi must be guaranteed. In this paper, LTE-U network planning and radio access optimization (subject to the presence of WiFi) has been addressed. Throughout our study, the need for accurate methods to characterize the radio propagation and appropriate interference models has been shown. In addition, it has been been verified that statistical system models provide means to efficiently determine network topologies that maximize the benefit from LTE-U and existing WiFi networks. This is necessary in the light of the large number of network topologies that need to be *compared*, which is not feasible by means of SLS. On the other hand, once statistically-optimized radio access topologies have been found, performance (e.g., capacity/QoS analysis) needs to be validated through SLS in order to take into account the features found in real systems, which cannot be modeled mathematically. The results also show the importance of reliable service demand models and statistics, in particular, load levels and spatial distribution, which have a profound impact on the resulting inter-system optimization, performance, and coexistence. The authors acknowledge that, as a novel approach to this difficult problem, several generalizations/refinements needs to be investigated. However, it should be remarked that effective planning and radio access optimization are not alternatives but **complementary tools** to increase the efficacy of other coexistence schemes, such as DCS, LBT, or DC. Current research efforts are aligned in that direction.

Acknowledgement

This work was supported by the project HII-ACTIVE: *High Impact Initiative - Advanced ConnecTIvity platform for VErtical segments* (EIT DIGITAL) and the Academy of Finland (grant 284811).

References

[1] Ericsson Research, *More than 50 billion connected devices*, 2011, available online at: www.ericsson.com.

[2] S. Rangan, T. Rappaport, and E. Erkip, "Millimeter-wave cellular wireless networks: potentials and challenges," *Proceedings of the IEEE*, vol. 102, no. 3, pp. 366–385, Mar. 2014.

[3] F. Abinader *et al*, "Enabling the coexistence of LTE and Wi-Fi in unlicensed bands," *IEEE Communications Magazine*, vol. 52, no. 11, pp. 54–61, Nov 2014.

[4] L. Verma *et al*, "WiFi on steroids: 802.11AC and 802.11AD," *IEEE Wireless Communications*, vol. 20, no. 6, pp. 30–35, Dec. 2013.

[5] R. Zhang, M. Wang, L. Cai, Z. Zheng, and X. Shen, "LTE-unlicensed: the future of spectrum aggregation for cellular networks," *IEEE Wireless Communications*, vol. 22, no. 3, pp. 150–159, Jun. 2015.

[6] A. Osseiran *et al*, "Scenarios for 5G mobile and wireless communications: the vision of the METIS project," *IEEE Communications Magazine*, vol. 52, no. 5, pp. 26–35, May 2014.

[7] M. R. Khawer, J. Tang, and F. Han, "usICIC - A Proactive Small Cell Interference Mitigation Strategy for Improving Spectral Efficiency of LTE Networks in the Unlicensed Spectrum," *IEEE Transactions on Wireless Communications*, vol. 15, no. 3, pp. 2303–2311, March 2016.

[8] H. Song and X. Fang, "A spectrum etiquette protocol and interference coordination for LTE in unlicensed bands (LTE-U)," in *Proc. 2015 IEEE Int. Conf. on Communication Wksp. (ICCW)*, June 2015, pp. 2338–2343.

[9] W. Xu *et al*, "Lower-complexity power allocation for LTE-U systems: a successive cap-limited waterfilling method," in *Proc. IEEE 81st Vehicular Technology Conference (VTC 2015 Spring)*, May 2015, pp. 1–6.

[10] H. Ko, J. Lee, and S. Pack, "A fair listen-before-talk algorithm for coexistence of LTE-U and WLAN," *IEEE Transactions on Vehicular Technology*, vol. PP, no. 99, pp. 1–1, 2016.

[11] A. Bhorkar, C. Ibars, and P. Zong, "Performance analysis of LTE and Wi-Fi in unlicensed band using stochastic geometry," in *Proc. 2014 IEEE 25th International Symposium on Personal, Indoor, and Mobile Radio Communication (PIMRC)*, Sept 2014, pp. 1310–1314.

[12] O. Sallent *et al*, "Learning-based coexistence for LTE operation in unlicensed bands," in *Proc. 2015 IEEE International Conference on Communication Wksp. (ICCW)*, June 2015, pp. 2307–2313.

[13] A. M. Voicu *et al*, "Coexistence of pico- and femto-cellular LTE-unlicensed with legacy indoor Wi-Fi deployments," in *Proc. 2015 IEEE Int. Conf. on Communication Wksp. (ICCW)*, June 2015, pp. 2294–2300.

[14] F. Chaves *et al*, "LTE UL power control for the improvement of LTE/Wi-Fi coexistence," in *Proc. IEEE 78th Vehicular Technology Conference (VTC 2013 Fall)*, Sept 2013, pp. 1–6.

[15] A. Sadek, T. Kadous, K. Tang, H. Lee, and M. Fan, "Extending LTE to unlicensed band - merit and coexistence," in *Proc. 2015 IEEE International Conf. on Communication Wksp. (ICCW)*, June 2015, pp. 2344–2349.

[16] C. Cano and D. Leith, "Coexistence of WiFi and LTE in unlicensed bands: a proportional fair allocation scheme," in *Proc. 2015 IEEE Int. Conf. on Communication Wksp. (ICCW)*, June 2015, pp. 2288–2293.

[17] C.-F. Yang, B.-C. Wu, and C.-J. Ko, "A ray-tracing method for modeling indoor wave propagation and penetration," *IEEE Transactions on Antennas and Propagation*, vol. 46, no. 6, pp. 907–919, Jun 1998.

[18] K. Haneda *et al*, "Spatial coexistence of millimeter-wave distributed indoor channels," in *Proc. IEEE 81st Vehicular Technology Conference (VTC 2015 Spring)*, May 2015, pp. 1–5.

[19] P. D. Marco, R. Chirikov, P. Amin, and F. Militano, "Coverage analysis of Bluetooth low energy and IEEE 802.11ah for office scenario," in *Proc. 2015 IEEE 26th International Symposium on Personal, Indoor, and Mobile Radio Communication (PIMRC)*, Aug 2015, pp. 2283–2287.

[20] J. Wu, Z. Zhang, Y. Hong, and Y. Wen, "Cloud radio access network (C-RAN): a primer," *IEEE Network*, vol. 29, no. 1, pp. 35–41, Jan 2015.

[21] T. Beitelmal and H. Yanikomeroglu, "A set cover based algorithm for Cell Switch-Off with different cell sorting criteria," in *Proc. 2014 IEEE Int. Conf. on Communication Wksp. (ICCW)*, June 2014, pp. 641–646.

[22] D. González G., H. Yanikomeroglu, M. García-Lozano, and S. R. Boqué, "A novel multiobjective framework for cell switch-off in dense cellular networks," in *Proc. 2014 IEEE Int. Conference on Communications (ICC)*, June 2014, pp. 2641–2647.

[23] U. Paul *et al*, "Understanding traffic dynamics in cellular data networks," in *Proc. 2011 IEEE International Conference on Computer Communications (INFOCOM)*, April 2011, pp. 882–890.

[24] D. Lee *et al*, "Spatial modeling of the traffic density in cellular networks," *IEEE Wireless Communications*, vol. 21, no. 1, pp. 80–88, Feb. 2014.

[25] D. González G. and J. Hämäläinen, "Topology and Irregularity in Cellular Networks," in *Proc. 2015 IEEE Wireless Communications and Networking Conference (WCNC)*, Mar. 2015, pp. 1731–1736.

[26] A. Papoulis and S. U. Pillai, *Probability, random variables, and stochastic processes*. Tata McGraw-Hill Education, 2002.

[27] Y. Sawaragi, I. Hirotaka, and T. Tanino, *Theory of Multiobjective Optimization*, 1st ed. Academic Press, Inc., 1985.

[28] C. A. Coello, G. B. Lamont, and D. A. Van Veldhuizen, *Evolutionary Algorithms for Solving Multi-Objective Problems*, 2nd ed. Springer: Genetic and Evolutionary Computation Series, 2007.

[29] K. Deb, A. Pratap, S. Agarwal, and T. Meyarivan, "A Fast and Elitist Multiobjective Genetic Algorithm: NSGA-II," *IEEE Transactions on Evolutionary Computation*, vol. 6, no. 2, pp. 182–197, Apr 2002.

[30] *WallMan: User reference guide, WinProp ProMan user reference and indoor scenarios*, AWE Communications GmbH, Online at: www.awe-communications.com.

[31] F. R. Marques *et al*, "Scheduling for improving system capacity in multiservice 3GPP LTE," *Journal of Electrical and Computer Engineering*, vol. 2010, no. 1, pp. 1–10, Jun. 2010.

[32] Group Radio Access Network, *TR 25.892: Feasibility Study for Orthogonal Frequency Division Multiplexing (OFDM) for UTRAN enhancement*, 3GPP, Jun 2004, v6.0.0.